

DOCUMENT CONTROL SHEET

	ORIGINATOR'S REF. NLR-TP-2003-123		SECURITY CLASS. Unclassified
ORIGINATOR National Aerospace Laboratory NLR, Amsterdam, The Netherlands			
TITLE Corrections for mirror sources in phased array processing techniques AIAA Paper 2003-3308			
PRESENTED AT The 9th AIAA/CEAS Aeroacoustics Conference as AIAA Paper 2003-3308, Hilton Head, South Carolina, USA, 12-14 May 2003			
AUTHORS P. Sijtsma and H. Holthusen	DATE March 2003	PP 13	REF 15
ABSTRACT When an aero-acoustic source is close to a reflecting wall, results from conventional phased array beamforming techniques are disturbed by the nearby mirror source, which is coherent with the original source. The recalculated source spectrum tends to deviate from the spectrum of the same source obtained in an anechoic environment. A periodic modulation of the spectrum occurs, which is most prominent at low frequencies. In this paper, a number of non-conventional beamforming techniques to correct for this spectral modulation is investigated. First, a technique is discussed which adds the mirror source to the transmission model. It was found that this technique is not very suitable because of its lack of robustness. Then, a more robust beamforming technique is proposed that minimises the influence of a given mirror source. By this technique, much better results were found. Nevertheless, at low frequencies the method still suffers from lack of robustness. Finally, a modification to this minimisation technique is proposed which preserves the robustness. Using this "controlled minimisation" technique, the best agreement was found between the recalculated spectra of a source close to a wall and the same source in anechoic conditions. The beamforming techniques were applied to array measurements on a calibration source in the DNW Low Speed Wind Tunnel LST.			



NLR-TP-2003-123

**Corrections for mirror sources in phased array
processing techniques**

AIAA Paper 2003-3308

P. Sijtsma and H. Holthusen*

* German Dutch Wind Tunnels

Presented as AIAA Paper 2003-3308 at the 9th AIAA/CEAS Aeroacoustics
Conference, Hilton Head, South Carolina, USA, 12-14 May 2003.

This report may be cited on condition that full credit is given to NLR and the authors.

Customer: National Aerospace Laboratory NLR
Working Plan number: A.2.A.3
Owner: National Aerospace Laboratory NLR
Division: Fluid Dynamics
Distribution: Unlimited
Classification title: Unclassified
March 2003

Approved by author:  27/03/03	Approved by project manager:  27/03/03	Approved by project managing department:  27/3/03
---	--	--



Contents

Nomenclature	3
I. Introduction	3
II. Preliminaries	4
Definitions	4
Vector-matrix notation	4
Beamforming	4
Conventional Beamforming	5
III. Formulation of the problem	5
Source measurements in DNW-LST	5
Application of Conventional Beamforming	6
IV. Analysis of the problem	6
Multiple sources	6
Conventional Beamforming with mirror sources	7
Spectral modulation	7
V. The Reflection Cancellor	8
VI. Minimisation of mirror source influence	9
Straightforward minimisation	9
Controlled minimisation	10
Extension to multiple mirror sources	11
VII. Concluding remarks	12
Effects of wind	12
Limits of application	12
Computation times	13
VIII. Conclusion	13
References	13
14 Figures	
(13 pages in total)	



CORRECTIONS FOR MIRROR SOURCES IN PHASED ARRAY PROCESSING TECHNIQUES

Pieter Sijtsma^{*}

National Aerospace Laboratory NLR, 8300 AD Emmeloord, The Netherlands

and

Hermann Holthusen[†]

German Dutch Wind Tunnels DNW-LLF, 8300 AD Emmeloord, The Netherlands

When an aero-acoustic source is close to a reflecting wall, results from conventional phased array beamforming techniques are disturbed by the nearby mirror source, which is coherent with the original source. The recalculated source spectrum tends to deviate from the spectrum of the same source obtained in an anechoic environment. A periodic modulation of the spectrum occurs, which is most prominent at low frequencies. In this paper, a number of non-conventional beamforming techniques to correct for this spectral modulation is investigated. First, a technique is discussed which adds the mirror source to the transmission model. It was found that this technique is not very suitable because of its lack of robustness. Then, a more robust beamforming technique is proposed that minimises the influence of a given mirror source. By this technique, much better results were found. Nevertheless, at low frequencies the method still suffers from lack of robustness. Finally, a modification to this minimisation technique is proposed which preserves the robustness. Using this “controlled minimisation” technique, the best agreement was found between the recalculated spectra of a source close to a wall and the same source in anechoic conditions. The beamforming techniques were applied to array measurements on a calibration source in the DNW Low Speed Wind Tunnel LST.

Nomenclature

a = source power
 c = speed of sound
 \mathbf{C} = cross-power matrix
 f = frequency (Hz)
 \mathbf{g} = steering vector
 \mathbf{G} = matrix of steering vectors
 i = imaginary unit
 K = number of sources
 N = number of microphones
 \mathbf{p} = vector of measured pressure amplitudes
 R_k = distance between source position and average microphone position
 \mathbf{x}_n = microphone position
 \mathbf{w} = weight vector
 ΔS = difference in path length

μ = control parameter
 $\boldsymbol{\lambda}$ = vector of Lagrange multipliers
 $\boldsymbol{\xi}_k$ = source position

I. Introduction

Microphone arrays become more and more in use as a tool for acoustic source location in wind tunnels, both in open^{1,2,3} and in closed test sections^{4,5}. Arrays in wind tunnels have proven their ability to quantify differences in sound source levels as a result of model modifications, using the Conventional Beamforming technique⁶. However, extraction of absolute acoustic source levels from wind tunnel array measurements is in general not possible by straightforward application of conventional methods.

In open test sections, the main difficulty is the presence of the wind tunnel shear layer between the wind tunnel model and the (out-of-flow) array. The shear layer causes loss of coherence between microphone signals, and, as a result, the beamforming process underpredicts the source levels. In fact, the predicted source levels become dependent on array size⁷. This problem (and also the problem of non-

^{*}Research Engineer, Aeroacoustics Department,
P.O. Box 153, e-mail: sijtsma@nlr.nl.

[†]P.O. Box 175, e-mail: hermann.holthusen@dnw.aero.

Copyright © 2003 by the National Aerospace Laboratory
NLR. Published by the American Institute of Aeronautics and
Astronautics, Inc. with permission.



compact sources) can be overcome by using an integration routine⁷.

In closed test sections, the main problem is the reverberation. When an acoustic source is too close to a wall, the source spectrum, reconstructed from array measurements, tends to deviate strongly from the free-field source spectrum⁵. This spectral distortion, which is due to the proximity of a mirror source, is the topic of this paper. A number of non-conventional beamforming techniques is evaluated for their suitability to correct for this spectral distortion.

First, the ‘‘Reflection Cancellation’’ technique, proposed by Guidati et al.⁸, is discussed, in which the mirror source is added to the transmission model. It will be argued that this method is not very suitable for correction of spectral distortion, because of its lack of robustness. Second, a correction technique similar to the inverse method of Nelson and Yoon^{9,10} is discussed, that minimises the array output from the mirror source direction. It will be concluded that this method performs better than the ‘‘Reflection Cancellation’’ technique. However, at low frequencies, this ‘‘Mirror Minimisation’’ technique also has its limitations with respect to robustness. Finally, a modification to the ‘‘Mirror Minimisation’’ technique is proposed, that preserves the robustness. The ‘‘amount of non-robustness’’ will be quantified by the ‘‘White Noise Gain’’. When the White Noise Gain of the ‘‘Mirror Minimisation’’ technique exceeds a certain prescribed value, an alternative method is used, in which the White Noise Gain is fixed.

The investigated correction techniques were applied to array measurements in the DNW Low Speed Wind Tunnel LST, on a calibration source¹¹ owned by NLR. This calibration source was designed to have a more or less uniform directivity. An array of 96 microphones, mounted in a sidewall, was used.

II. Preliminaries

Definitions

A Cartesian co-ordinate system is used, in which an array of N microphones is considered, located in $\mathbf{x}_n = (x_n, y_n, z_n)$, where n runs from 1 to N . Each microphone measures a fluctuating pressure signal $\chi_n(t)$. Microphone spectra (single-sided) can be obtained by performing Fourier transforms over a finite time interval, like:

$$p_n(f) = \frac{2}{T} \int_0^T \psi(t) \chi_n(t) e^{-2\pi i f t} dt, \quad (1)$$

in which f is the frequency and $\psi(t)$ is an optional ‘‘window’’ function, e.g. the Hanning window⁹. Microphone auto-spectra $C_{nn}(f)$ are calculated by:

$$C_{nn}(f) = \frac{1}{2} \langle \|p_n(f)\|^2 \rangle = \frac{1}{2} \langle p_n(f) p_n^*(f) \rangle, \quad (2)$$

where the asterisk denotes complex conjugation and $\langle \dots \rangle$ means averaging over a number of time intervals, as in Eq. (1). Array cross-spectra are defined by:

$$C_{mn}(f) = \frac{1}{2} \langle p_m(f) p_n^*(f) \rangle. \quad (3)$$

Vector-matrix notation

From now on, we will write the relevant quantities as vectors and matrices. Furthermore, for brevity, we will omit the frequency dependence ‘‘(f)’’. This means that the ‘‘pressure amplitudes’’, Eq. (1), are put in an N -dimensional vector \mathbf{p} :

$$\mathbf{p} = \begin{pmatrix} p_1(f) \\ \vdots \\ p_N(f) \end{pmatrix}. \quad (4)$$

Furthermore, the $N \times N$ cross-power matrix \mathbf{C} is introduced by:

$$\mathbf{C} = \frac{1}{2} \langle \mathbf{p} \mathbf{p}^* \rangle, \quad (5)$$

where the asterisk now means ‘‘complex conjugate transpose’’.

Beamforming

The process of source location (beamforming) can be written symbolically as:

$$a = \mathbf{w}^* \mathbf{C} \mathbf{w}, \quad (6)$$

where \mathbf{w} is an N -dimensional weight vector that is dependent on an assumed source direction (viz. a point in the scan grid) and a is the resulting source power for that source direction. The weight vector has to be such that unit gain is found for unit sources in the assumed direction:

$$\mathbf{w}^* \mathbf{g} = 1. \quad (7)$$



Herein, \mathbf{g} is the “steering vector”, consisting of microphone pressure amplitudes, induced by a unit source. For instance if monopole sources are assumed, \mathbf{g} consists of elements:

$$g_n = \frac{-1}{4\pi R_n} \exp\left[-\frac{2\pi if}{c} R_n\right], \quad (8)$$

where c is the speed of sound and R_n is the distance between source and n -th microphone.

It may be advantageous to exclude the auto-powers C_{nn} from the beamforming process, if the microphones contain much self-noise¹².

Conventional Beamforming

The weight vector for the Conventional Beamforming technique is found by minimising

$$J(\mathbf{w}) = \frac{1}{2} \mathbf{w}^* \mathbf{w} = \frac{1}{2} \|\mathbf{w}\|^2, \quad (9)$$

under the constraint

$$\mathbf{w}^* \mathbf{g} = 1. \quad (10)$$

The solution of this constrained optimisation problem is:

$$\mathbf{w} = \frac{\mathbf{g}}{\mathbf{g}^* \mathbf{g}}. \quad (11)$$

Hence, the array output (6) is:

$$a = \frac{\mathbf{g}^* \mathbf{C} \mathbf{g}}{(\mathbf{g}^* \mathbf{g})^2}. \quad (12)$$

It is noted that the same array output as (12) is found when the following expression is minimised:

$$J(a) = \|\mathbf{C} - a \mathbf{g} \mathbf{g}^*\|^2 \quad (13)$$

Since Eq. (9) is minimised, the Conventional Beamforming technique is the most robust method available. That is, inaccuracies in source characteristics (i.e., steering vector \mathbf{g}), in source position or in microphone calibrations lead to the smallest possible errors in the array output (6). Moreover, there is not much sensitivity to noise.

Therefore, the Conventional Beamforming technique is very suitable for wind tunnel measurements.

III. Formulation of the problem

Source measurements in DNW-LST

To investigate reverberation effects in the DNW Low Speed Wind Tunnel LST, array measurements were carried out with the NLR calibration source¹¹. An array of 1 m diameter was used, consisting of 96 microphones, which was mounted in a sidewall. Many variations were made on source position, array position and wind speed. To reduce the effects of reflections from the wall opposite to the array, this wall was lined with a layer of porous material covered by a perforate plate.

The objective was to compare beamforming results with the source spectrum measured in an anechoic room. However, for unknown reason, this anechoic source spectrum appeared to be significantly different, both in shape and in level, from the source spectra in the DNW-LST. Moreover, a reference transducer inside the calibration source was out of order during the tests in the DNW-LST. Hence, it was impossible to compare with anechoic data. On the other hand, all source spectra derived from the DNW-LST measurements appeared to be variations on the source spectrum obtained with the source in the centre of the tunnel. Therefore, this tunnel centre source spectrum was used as a “datum” that is considered to be representative for anechoic conditions (which, of course, does not hold for low frequencies).

In this paper, we consider only measurements without wind, with the array positioned at mid-height in a sidewall, and with the source at (0,0,0.8), which is 80 cm above the tunnel centre (0,0,0). The test section of the DNW-LST is 3.0 m wide and 2.22 m high. A sketch is shown in Fig. 1.

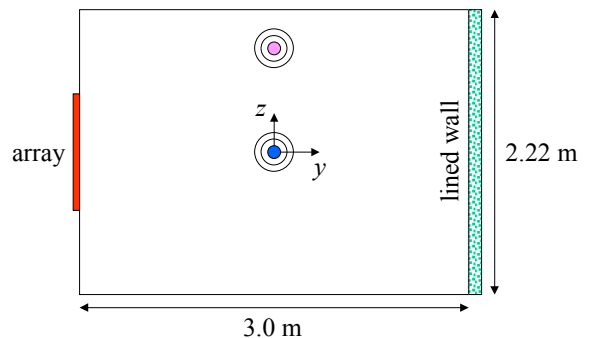


Fig. 1 Set-up of array measurements in DNW-LST



Application of Conventional Beamforming

Typical 1/3 octave band acoustic images, obtained by applying Conventional Beamforming on a vertical plane of 60x60 cm² surrounding the source position at (0,0,0.8), are shown in Fig. 2. In Fig. 3, similar plots are shown for the source in the datum position (0,0,0). The dynamic range of the source plots is 13 dB. The colour levels are obtained by auto-scaling.

When the source is in the tunnel centre (Fig. 3), the source position is clearly visible as the peak level locations. When the source is in (0,0,0.8), this is only true for frequencies above 2000 Hz. Below that frequency, the influence of the mirror source at (0,0,1.42) is too strong.

Next, we consider source spectra: narrow-band beamforming results obtained by focusing on the source positions. In Fig. 4, the source spectra, obtained by Conventional Beamforming, of the source positions (0,0,0.8) and (0,0,0) are compared. The spectra are presented as recalculated SPL at 1 m from the source. The agreement is good at high frequencies, but at low frequencies, a modulation on the (0,0,0.8) spectrum appears. In fact, a similar modulation is found by simulations, i.e., when coherent sources (at unit strength) are simulated in (0,0,0.8) and (0,0,1.42). This is shown in Fig. 5. In the next section this phenomenon of spectral modulation is analysed.

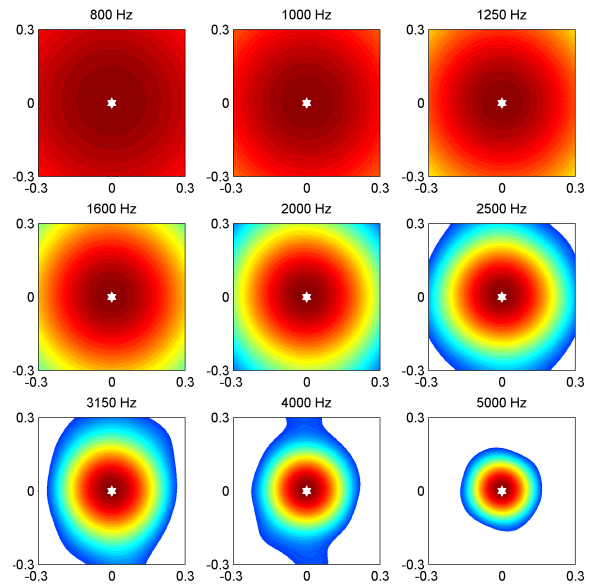


Fig. 3 Acoustic images, source in (0,0,0), obtained by Conventional Beamforming

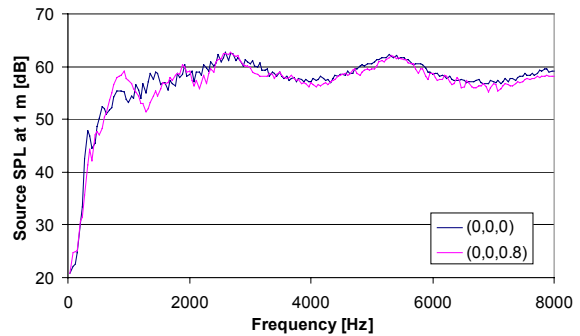


Fig. 4 Source spectra, obtained by Conventional Beamforming

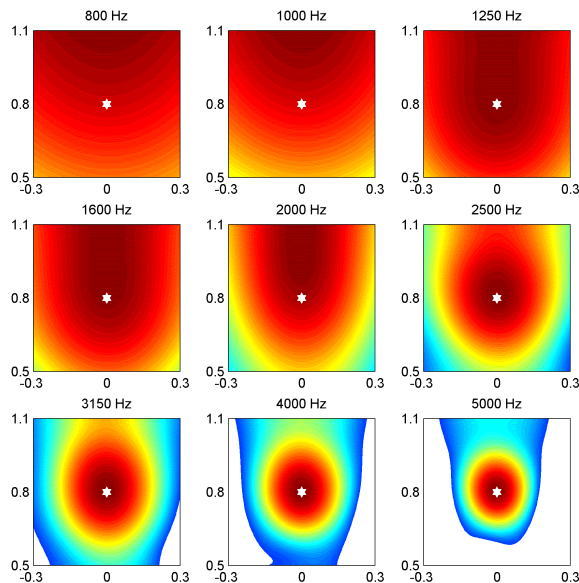


Fig. 2 Acoustic images, source in (0,0,0.8), obtained by Conventional Beamforming

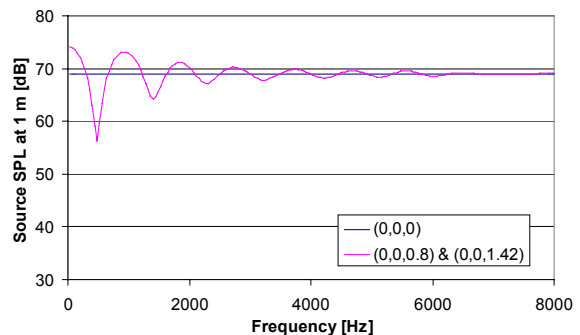


Fig. 5 Simulated source spectra, obtained by Conventional Beamforming

IV. Analysis of the problem

Multiple sources

Suppose there are K sources, resulting in pressure amplitude vectors \mathbf{p} "built up" by K components:



$$\mathbf{p} = \sum_{k=1}^K \mathbf{p}_k. \quad (14)$$

For the cross-power matrix, we have

$$\mathbf{C} = \frac{1}{2} \left\langle \left(\sum_{k=1}^K \mathbf{p}_k \right) \left(\sum_{k=1}^K \mathbf{p}_k \right)^* \right\rangle = \frac{1}{2} \sum_{k=1}^K \sum_{l=1}^K \langle \mathbf{p}_k \mathbf{p}_l^* \rangle. \quad (15)$$

Hence the array output (6) is given by the double summation:

$$a = \sum_{k=1}^K \sum_{l=1}^K \mathbf{w}^* \frac{1}{2} \langle \mathbf{p}_k \mathbf{p}_l^* \rangle \mathbf{w}. \quad (16)$$

If the source components are incoherent, then the cross-products $\mathbf{p}_k \mathbf{p}_l^*$ have random phase and will therefore disappear by averaging. Then, in the limit the single summation remains:

$$a = \sum_{k=1}^K \mathbf{w}^* \frac{1}{2} \langle \mathbf{p}_k \mathbf{p}_k^* \rangle \mathbf{w}. \quad (17)$$

However, if sources are each other's mirror, they are coherent¹⁴. In that case (17) does not hold.

Conventional Beamforming with mirror sources

Consider a pair of coherent unit point sources:

$$\mathbf{p}_k = \mathbf{g}_k, \quad k=1,2, \quad (18)$$

The pressure vector \mathbf{p}_1 may be induced by a real source in ξ_1 , while \mathbf{p}_2 is induced by its mirror source in ξ_2 . Application of the Conventional Beamforming technique, (16) with (11), to the cross-power matrix induced by the mirror sources of (18), leads to

$$a = \frac{1}{2} + \frac{\text{Re}(\mathbf{g}_1^* \mathbf{g}_2)}{\mathbf{g}_1^* \mathbf{g}_1} + \frac{|\mathbf{g}_1^* \mathbf{g}_2|^2}{2(\mathbf{g}_1^* \mathbf{g}_1)^2}. \quad (19)$$

The first term in the right hand side of (19) is the desired answer, so the other terms are errors. The last term in the right hand side of (19) is small compared to the second term, so the second term is probably the cause for the spectral distortion. (If the sources were incoherent, the second term in the right hand side of (19) would disappear.)

Spectral modulation

If \mathbf{g}_1 and \mathbf{g}_2 are given by Eq. (8), hence if

$$\mathbf{g}_{k,n} = \frac{-1}{4\pi R_{k,n}} \exp\left[-\frac{2\pi i f R_{k,n}}{c}\right], \quad k=1,2, \quad (20)$$

with

$$R_{k,n} = \|\xi_k - \mathbf{x}_n\|, \quad (21)$$

then we have for the main error term in (19):

$$\frac{\text{Re}(\mathbf{g}_1^* \mathbf{g}_2)}{\mathbf{g}_1^* \mathbf{g}_1} = \frac{1}{\mathbf{g}_1^* \mathbf{g}_1} \text{Re} \left(\sum_{n=1}^N \frac{1}{(4\pi)^2 R_{1,n} R_{2,n}} \times \exp\left[\frac{2\pi i f}{c}(R_{1,n} - R_{2,n})\right] \right). \quad (22)$$

If the sources ξ_1 and ξ_2 are not in the near field of the array $\{\mathbf{x}_n, n=1, \dots, N\}$, then we have:

$$\begin{aligned} \frac{\text{Re}(\mathbf{g}_1^* \mathbf{g}_2)}{\mathbf{g}_1^* \mathbf{g}_1} &\approx \text{Re} \left(\exp\left[\frac{2\pi i f}{c}(\bar{R}_1 - \bar{R}_2)\right] \right) \\ &= \cos\left(\frac{2\pi f}{c}(\bar{R}_1 - \bar{R}_2)\right), \end{aligned} \quad (23)$$

where \bar{R}_k is the distance between the source location ξ_k and the average microphone location $\langle \mathbf{x}_n \rangle$. In other words, the error made in the Conventional Beamforming algorithm is dependent on frequency and it alternates like

$$\text{Error}(f) \propto \cos[2\pi f \Delta S / c], \quad (24)$$

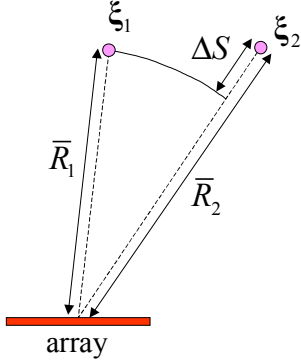
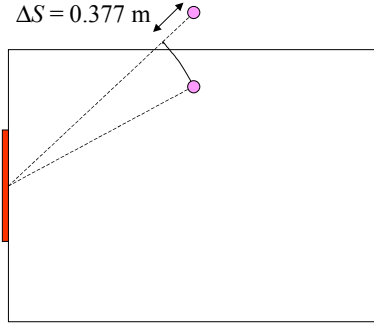
where

$$\Delta S = \bar{R}_1 - \bar{R}_2, \quad (25)$$

which is the difference in path length between sources and array (see Fig. 6). Hence, the "period" of the perturbation is

$$\Delta f = c / \Delta S. \quad (26)$$

This agrees with the results of Fig. 4 and Fig. 5, where we have $\Delta S = 0.377$ m (see Fig. 7) and, hence, $\Delta f \approx 900$ Hz.

Fig. 6 Definition of ΔS Fig. 7 Source in $(0,0,0.8)$ and mirror source in $(0,0,1.42)$

V. The Reflection Canceller

To cancel out the effect of coherent (mirror) sources, Guidati et al.⁸ proposed to include them in the steering vector. In the case of two point sources, the steering vector becomes:

$$\mathbf{g} = \mathbf{g}_1 + \mathbf{g}_2. \quad (27)$$

Hence, the weight vector for Conventional Beamforming is

$$\mathbf{w} = \frac{\mathbf{g}_1 + \mathbf{g}_2}{(\mathbf{g}_1 + \mathbf{g}_2)^* (\mathbf{g}_1 + \mathbf{g}_2)} \quad (28)$$

and the expression for the array output becomes:

$$a = \frac{(\mathbf{g}_1^* + \mathbf{g}_2^*) \mathbf{C} (\mathbf{g}_1 + \mathbf{g}_2)}{\left((\mathbf{g}_1 + \mathbf{g}_2)^* (\mathbf{g}_1 + \mathbf{g}_2) \right)^2}. \quad (29)$$

If we write, as in the previous section,

$$\mathbf{p}_k = \mathbf{g}_k, \quad k = 1, 2, \quad (30)$$

and, consequently,

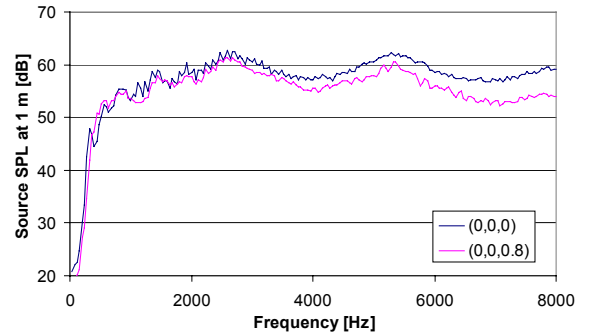
$$\begin{aligned} \mathbf{C} &= \frac{1}{2} (\mathbf{g}_1 + \mathbf{g}_2) (\mathbf{g}_1^* + \mathbf{g}_2^*) \\ &= \frac{1}{2} \{ \mathbf{g}_1 \mathbf{g}_1^* + \mathbf{g}_1 \mathbf{g}_2^* + \mathbf{g}_2 \mathbf{g}_1^* + \mathbf{g}_2 \mathbf{g}_2^* \}, \end{aligned} \quad (31)$$

then (29) is worked out as

$$a = \frac{(\mathbf{g}_1^* + \mathbf{g}_2^*) (\mathbf{g}_1 + \mathbf{g}_2) (\mathbf{g}_1^* + \mathbf{g}_2^*) (\mathbf{g}_1 + \mathbf{g}_2)}{2 \left((\mathbf{g}_1 + \mathbf{g}_2)^* (\mathbf{g}_1 + \mathbf{g}_2) \right)^2} = \frac{1}{2}, \quad (32)$$

which is the desired answer.

This ‘‘Reflection Canceller’’ technique was applied to the measurements with the source in $(0,0,0.8)$. Narrow-band beamforming results, compared with the datum results at $(0,0,0)$, are shown in Fig. 8. Compared with Fig. 4, the agreement at low frequencies is much better. However, at higher frequencies, the agreement is worse. The increasing disagreement at higher frequencies is a consequence of the lack of robustness of the Reflection Canceller. This will be explained in the following.

Fig. 8 Source spectra; the $(0,0,0.8)$ spectrum is obtained by the Reflection Canceller with mirror source in $(0,0,1.42)$

Suppose there is a mismatch between assumed and actual mirror source, say

$$\mathbf{p}_2 = e^{i\varphi} \mathbf{g}_2. \quad (33)$$

Then we have, instead of (32):

$$a = \frac{(\mathbf{g}_1^* + \mathbf{g}_2^*) (\mathbf{g}_1 + e^{i\varphi} \mathbf{g}_2) (\mathbf{g}_1^* + e^{-i\varphi} \mathbf{g}_2^*) (\mathbf{g}_1 + \mathbf{g}_2)}{2 \left((\mathbf{g}_1 + \mathbf{g}_2)^* (\mathbf{g}_1 + \mathbf{g}_2) \right)^2}. \quad (34)$$



It is obvious that phase errors φ can lead to large errors in the source power a . Phase errors φ are easily made. For example, a phase error $\varphi = \pi/4$ (45°) corresponds, at 5000 Hz, to a distance error of less than 1 cm. Moreover, errors in absolute value are possible too, for example when the reflection is not 100% or if a wrong assumption is made for the source directivity.

Another comment on the Reflection Canceller is that it is similar to beamforming with inclusion of the mirror array. This becomes clear when we rewrite (29) as

$$a = \frac{\begin{pmatrix} \mathbf{g}_1 \\ \mathbf{g}_2 \end{pmatrix}^* \begin{pmatrix} \mathbf{C} & \mathbf{C} \\ \mathbf{C} & \mathbf{C} \end{pmatrix} \begin{pmatrix} \mathbf{g}_1 \\ \mathbf{g}_2 \end{pmatrix}}{\left(\begin{pmatrix} \mathbf{g}_1 + \mathbf{g}_2 \end{pmatrix}^* \begin{pmatrix} \mathbf{g}_1 + \mathbf{g}_2 \end{pmatrix} \right)^2}. \quad (35)$$

An illustration is sketched in Fig. 9. The effective array (array + mirror array), however, will not have an optimal microphone arrangement. Unusual beam patterns will be the result, with high side lobe levels, unless the presence of the mirror array is taken into account in the array design.

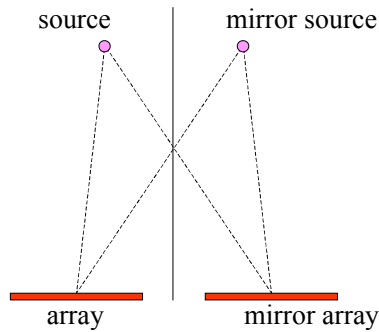


Fig. 9 Equivalence of mirror source and mirror array

The source plots for this case (source in $(0,0,0.8)$) are drawn in Fig. 10. Strong variations in source levels are observed. Moreover, for frequencies below 4000 Hz, the level at $(0,0,0.8)$ is far below the peak level in the plots. It is clear that a very accurate knowledge of the source position is required, before the Reflection Canceller can be applied to the calculation of source spectra.

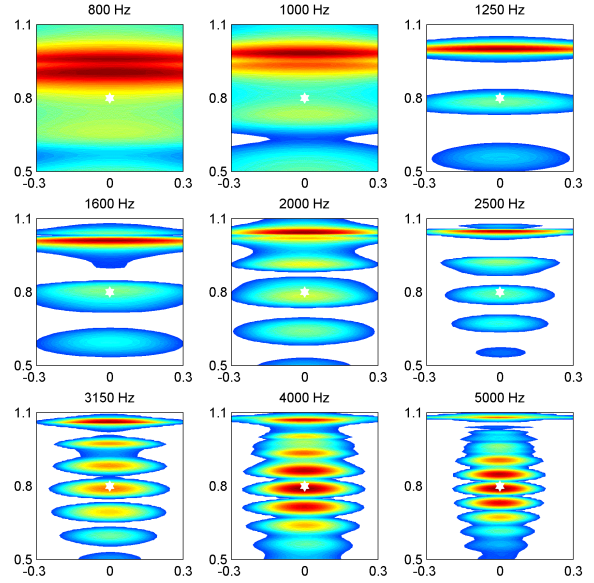


Fig. 10 Acoustic images, source in $(0,0,0.8)$, obtained by the Reflection Canceller with mirror source in $(0,0,1.42)$

VI. Minimisation of mirror source influence

Straightforward minimisation

Recalling that the weight vector for Conventional Beamforming is the result of minimising Eq. (9) under the constraint (10), we now propose a beamforming method that, again, minimises Eq. (9), but now under two constraints:

$$\mathbf{w}^* \mathbf{g}_1 = 1 \text{ and } \mathbf{w}^* \mathbf{g}_2 = 0, \quad (36)$$

where \mathbf{g}_1 corresponds to a source in ξ_1 and \mathbf{g}_2 to its mirror in ξ_2 . If we use, again, Eq. (18) to describe the input, then the array output becomes:

$$a = \frac{1}{2} \mathbf{w}^* \{ \mathbf{g}_1 \mathbf{g}_1^* + \mathbf{g}_1 \mathbf{g}_2^* + \mathbf{g}_2 \mathbf{g}_1^* + \mathbf{g}_2 \mathbf{g}_2^* \} \mathbf{w} = \frac{1}{2} \left\{ |\mathbf{w}^* \mathbf{g}_1|^2 + (\mathbf{w}^* \mathbf{g}_1)(\mathbf{w}^* \mathbf{g}_2)^* + (\mathbf{w}^* \mathbf{g}_2)(\mathbf{w}^* \mathbf{g}_1)^* + |\mathbf{w}^* \mathbf{g}_2|^2 \right\} = \frac{1}{2}. \quad (37)$$

In contrast with the Reflection Canceller, this approach also provides good answers when there is less than 100% reflection from the mirror source. Moreover, this method should be less sensitive to assumed source position.



The solution of the minimisation problem (9) with (36) can be found with the method of Lagrange multipliers, i.e., by introducing multipliers λ_1 and λ_2 , and by minimising

$$J(\mathbf{w}) = \frac{1}{2} \mathbf{w}^* \mathbf{w} - \lambda_1 \mathbf{w}^* \mathbf{g}_1 - \lambda_2 \mathbf{w}^* \mathbf{g}_2 \quad (38)$$

as if there were no constraints. The solution is

$$\mathbf{w} = \lambda_1 \mathbf{g}_1 + \lambda_2 \mathbf{g}_2. \quad (39)$$

The multipliers λ_1 and λ_2 then follow from (36):

$$\begin{cases} \mathbf{g}_1^* \mathbf{g}_1 \lambda_1 + \mathbf{g}_1^* \mathbf{g}_2 \lambda_2 = 1, \\ \mathbf{g}_2^* \mathbf{g}_1 \lambda_1 + \mathbf{g}_2^* \mathbf{g}_2 \lambda_2 = 0, \end{cases} \quad (40)$$

which can be written in matrix format:

$$\begin{pmatrix} \mathbf{g}_1^* \mathbf{g}_1 & \mathbf{g}_1^* \mathbf{g}_2 \\ \mathbf{g}_2^* \mathbf{g}_1 & \mathbf{g}_2^* \mathbf{g}_2 \end{pmatrix} \begin{pmatrix} \lambda_1 \\ \lambda_2 \end{pmatrix} = \begin{pmatrix} 1 \\ 0 \end{pmatrix}. \quad (41)$$

Hence,

$$\begin{pmatrix} \lambda_1 \\ \lambda_2 \end{pmatrix} = \begin{pmatrix} \mathbf{g}_1^* \mathbf{g}_1 & \mathbf{g}_1^* \mathbf{g}_2 \\ \mathbf{g}_2^* \mathbf{g}_1 & \mathbf{g}_2^* \mathbf{g}_2 \end{pmatrix}^{-1} \begin{pmatrix} 1 \\ 0 \end{pmatrix}. \quad (42)$$

The weight vector \mathbf{w} then follows from insertion of (42) into (39).

This ‘‘Mirror Minimisation’’ technique was applied to the measurements with the source in (0,0,0.8). The source plots, which were obtained by varying ξ_1 and keeping ξ_2 fixed at the mirror position (0,0,1.42), are shown in Fig. 11. As in Fig. 2, the source position only coincides with the peak level locations at frequencies higher than 2000 Hz. Nevertheless, Fig. 11 shows that there is much less sensitivity to assumed source position than with the Reflection Canceller (cf. Fig. 10).

In Fig. 12 the source spectrum is compared to the datum source spectrum. As expected, the agreement is good. The modulation of Fig. 4 has disappeared, and the agreement at high frequencies is much better than in Fig. 8.

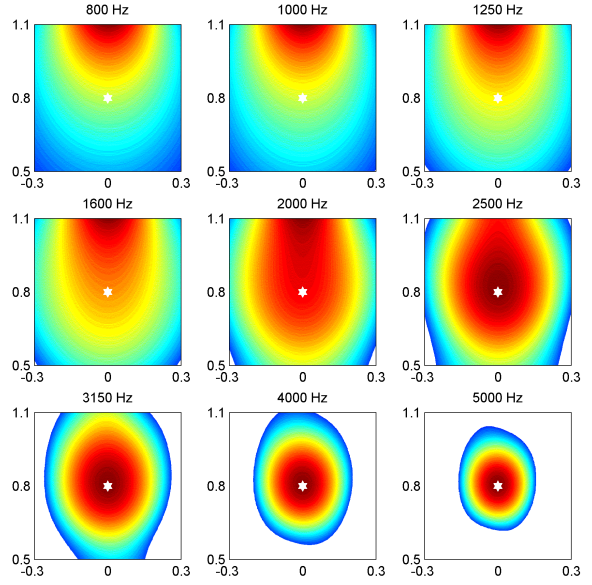


Fig. 11 Acoustic images, source in (0,0,0.8), obtained by Mirror Minimisation with mirror source in (0,0,1.42)

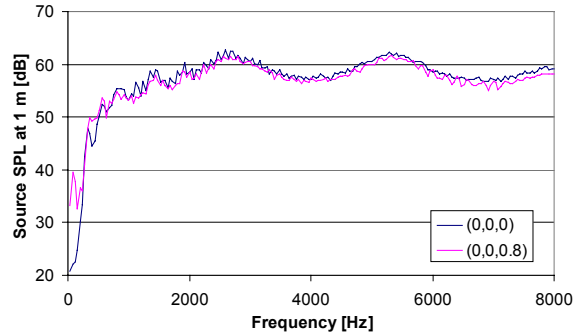


Fig. 12 Source spectra; the (0,0,0.8) spectrum is obtained by Mirror Minimisation with mirror source in (0,0,1.42)

Only at frequencies below 500 Hz, there is significant difference between both spectra in Fig. 12. This is mainly due to the fact that the matrix in (42) becomes ill-conditioned for those frequencies. As a result, the weight vector \mathbf{w} may become too large, thus making the method non-robust. To overcome this, a modification of the ‘‘Mirror Minimisation’’ technique is proposed below.

Controlled minimisation

To control the robustness of the method, we introduce the ‘‘White Noise Gain’’. ‘‘White noise’’ means here $\mathbf{C} = \mathbf{I}$, where \mathbf{I} is the identity matrix. The ‘‘White Noise Gain’’ is the array output (6) for ‘‘white noise’’:

$$a = \mathbf{w}^* \mathbf{I} \mathbf{w} = \mathbf{w}^* \mathbf{w}. \quad (43)$$



This White Noise Gain is compared with the minimum White Noise Gain, obtained with Conventional Beamforming, Eq. (11):

$$a = \left(\frac{\mathbf{g}_1}{\mathbf{g}_1^* \mathbf{g}_1} \right)^* \left(\frac{\mathbf{g}_1}{\mathbf{g}_1^* \mathbf{g}_1} \right) = \frac{1}{\mathbf{g}_1^* \mathbf{g}_1}. \quad (44)$$

The ‘‘White Noise Gain Constraint’’ WNC¹⁵ is then defined by the ratio between (43) and (44), expressed in dB:

$$\text{WNC} = 10^{10} \log \left[(\mathbf{w}^* \mathbf{w}) (\mathbf{g}_1^* \mathbf{g}_1) \right]. \quad (45)$$

By definition, we have WNC = 0 for Conventional Beamforming and WNC > 0 otherwise.

The ‘‘Controlled Mirror Minimisation’’ technique is now defined as follows. First, the straightforward Mirror Minimisation technique is applied, and the WNC is calculated. If the WNC exceeds a certain prescribed value, say a few dB, then the solution given by (39) and (42) is rejected. As alternative, we then minimise

$$\begin{aligned} J(\mathbf{w}) &= \frac{1}{2} \left\{ (1-\mu) \mathbf{w}^* \mathbf{w} + \mu |\mathbf{w}^* \mathbf{g}_2|^2 \right\} \\ &= \frac{1}{2} \mathbf{w}^* \left[(1-\mu) \mathbf{I} + \mu \mathbf{g}_2^* \mathbf{g}_2 \right] \mathbf{w}, \end{aligned} \quad (46)$$

under the single constraint

$$\mathbf{w}^* \mathbf{g}_1 = 1. \quad (47)$$

In (46), μ is a control parameter to be chosen such that the WNC attains the prescribed value. The solution of the optimisation problem is

$$\mathbf{w} = \frac{\left[(1-\mu) \mathbf{I} + \mu \mathbf{g}_2^* \mathbf{g}_2 \right]^{-1} \mathbf{g}_1}{\mathbf{g}_1^* \left[(1-\mu) \mathbf{I} + \mu \mathbf{g}_2^* \mathbf{g}_2 \right]^{-1} \mathbf{g}_1}. \quad (48)$$

For $\mu = 0$, when the method is identical to the Conventional Beamforming technique, we have WNC = 0. For increasing μ , the WNC will increase also. For μ somewhere between 0 and 1, the WNC will attain the prescribed value. This μ is searched numerically.

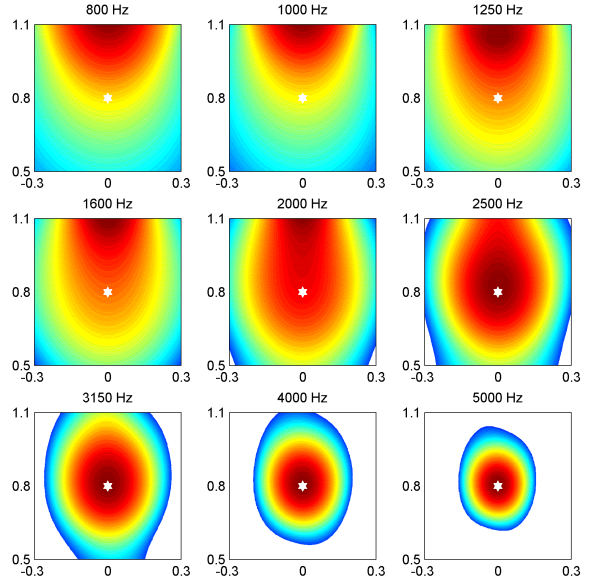


Fig. 13 Acoustic images, source in $(0,0,0.8)$, obtained by Controlled Mirror Minimisation with mirror source in $(0,0,1.42)$

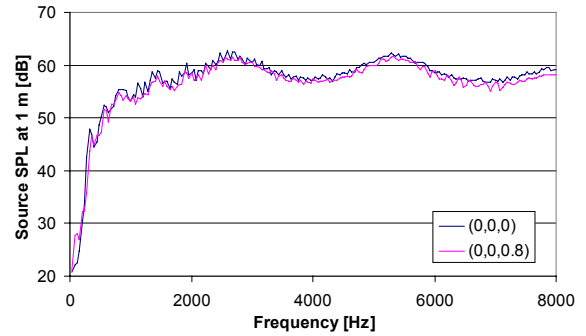


Fig. 14 Source spectra; the $(0,0,0.8)$ spectrum is obtained by Controlled Mirror Minimisation with mirror source in $(0,0,1.42)$

Result with the Controlled Mirror Minimisation technique, with WNC = 5 dB, are shown in Fig. 13 (source plots) and Fig. 14 (source spectra). Only for low frequencies, the results are different from the results of the straightforward Mirror Minimisation method (Fig. 11 and Fig. 12). The Controlled Mirror Minimisation technique does not provide more accurate source locations (Fig. 13), but the source spectrum now agrees very well with the $(0,0,0)$ spectrum, including the low-frequency part (Fig. 14).

Extension to multiple mirror sources

The extension of the method to multiple mirror sources is straightforward. Suppose that mirror sources are located in ξ_k , $k = 2, \dots, K$ with associated



steering vectors $\mathbf{g}_k, k = 2, \dots, K$. Then the problem is to minimise $J(\mathbf{w})$, Eq. (9), under the constraint:

$$\mathbf{G}^* \mathbf{w} = \mathbf{b}, \quad (49)$$

where \mathbf{G} is an $N \times K$ matrix, of which the columns consist of the steering vectors,

$$\mathbf{G} = (\mathbf{g}_1 \quad \dots \quad \mathbf{g}_K), \quad (50)$$

and \mathbf{b} is a K -dimensional vector defined by:

$$b_k = \begin{cases} 1, & k = 1, \\ 0, & k \geq 2. \end{cases} \quad (51)$$

The equivalent expression to minimise, with Lagrange multipliers, becomes:

$$J(\mathbf{w}) = \frac{1}{2} \mathbf{w}^* \mathbf{w} - \mathbf{w}^* \mathbf{G} \boldsymbol{\lambda}, \quad (52)$$

where $\boldsymbol{\lambda}$ is now a K -dimensional vector. The solution is

$$\mathbf{w} = \mathbf{G} \boldsymbol{\lambda}. \quad (53)$$

Solving the Lagrange multiplier $\boldsymbol{\lambda}$ from (49) yields:

$$\mathbf{w} = \mathbf{G} (\mathbf{G}^* \mathbf{G})^{-1} \mathbf{b}. \quad (54)$$

Then, the array output is

$$a = \mathbf{b}^* (\mathbf{G}^* \mathbf{G})^{-1} \mathbf{G}^* \mathbf{C} \mathbf{G} (\mathbf{G}^* \mathbf{G})^{-1} \mathbf{b}. \quad (55)$$

Expression (55) is analogous to the inverse method of Nelson and Yoon^{9,10}, in which the following expression is minimised:

$$J(\mathbf{A}) = \|\mathbf{C} - \mathbf{G} \mathbf{A} \mathbf{G}^*\|^2, \quad (56)$$

where \mathbf{A} is a $K \times K$ matrix containing the cross-powers of the K unknown sources. The solution is:

$$\mathbf{A} = (\mathbf{G}^* \mathbf{G})^{-1} \mathbf{G}^* \mathbf{C} \mathbf{G} (\mathbf{G}^* \mathbf{G})^{-1}. \quad (57)$$

Comparing Eq. (55) with Eq. (57), it is concluded that expression (55) is just the source auto-power of the first source, i.e., $a = A_{11}$.

For ‘‘Controlled Mirror Minimisation’’, which is applied when the WNC, (45), becomes too large because the matrix $\mathbf{G}^* \mathbf{G}$ becomes ill-conditioned, we minimise

$$J(\mathbf{w}) = \frac{1}{2} \left\{ (1 - \mu) \mathbf{w}^* \mathbf{w} + \mu \sum_{k=2}^K |\mathbf{w}^* \mathbf{g}_k|^2 \right\} \\ = \frac{1}{2} \mathbf{w}^* \left[(1 - \mu) \mathbf{I} + \mu \sum_{k=2}^K \mathbf{g}_k \mathbf{g}_k^* \right] \mathbf{w}, \quad (58)$$

again under the constraint (47). The solution of this optimisation problem is

$$\mathbf{w} = \frac{\left[(1 - \mu) \mathbf{I} + \mu \sum_{k=2}^K \mathbf{g}_k \mathbf{g}_k^* \right]^{-1} \mathbf{g}_1}{\mathbf{g}_1^* \left[(1 - \mu) \mathbf{I} + \mu \sum_{k=2}^K \mathbf{g}_k \mathbf{g}_k^* \right]^{-1} \mathbf{g}_1}. \quad (59)$$

It is noted that this approach of obtaining robust solutions is different from the approach of Nelson and Yoon^{9,10}, who consider regularisation techniques for the matrix $\mathbf{G}^* \mathbf{G}$.

VII. Concluding remarks

Effects of wind

The beamforming techniques described in this paper are applied only to source measurements without wind. Nevertheless, the authors expect the (Controlled) Mirror Minimisation method to work just as well in case of wind. Exclusion of the main diagonal from the cross-power matrix, which is needed when the signal to noise ratio is low, is not expected to be harmful. However, the method could not be applied to measurements of the ‘‘monopole’’ calibration source with wind, because the source level was too low compared to the microphone self noise induced by the wind tunnel boundary layer. At $M = 0.2$, and for frequencies below 5000 Hz, the source level was more than 20 dB below the microphone self noise level. This difference is too much to get meaningful beamforming results, even with exclusion of the auto-powers.

Limits of application

The (Controlled) Mirror Minimisation method performs well if the matrix in Eq. (41) has a low condition number (ratio between highest and lowest eigenvalue). This is true when the steering vectors \mathbf{g}_1 and \mathbf{g}_2 are well independent, in other words, when

$$\|\mathbf{g}_1 \mathbf{g}_2\| / \|\mathbf{g}_1\| \|\mathbf{g}_2\| \ll 1. \quad (60)$$



The method performs less when (60) comes close to unity, i.e., when \mathbf{g}_1 and \mathbf{g}_2 become more and more dependent. This occurs (a) at low frequencies, (b) when a source is close to a wall and, hence, close to its mirror, and (c) when the array, the source and its mirror are in one line (reflection by the wall opposite to the array).

Computation times

The straightforward Mirror Minimisation method needs about 40% more computing time than the Conventional Beamforming method, which makes it feasible as an alternative. However, the Controlled Mirror Minimisation method needs 10 to 20 times more computing time, due to the iterative search process for the control parameter μ . Therefore, this method should be used after the standard array processing, and applied to single source points, as a tool to improve source spectra.

VIII. Conclusion

When an acoustic source is too close to a wall, the source spectrum, reconstructed from array measurements using the Conventional Beamforming technique, tends to deviate strongly from the corresponding free-field source spectrum. The free-field source spectrum appears to be disturbed by a periodic modulation, due to the proximity of a mirror source.

A study was performed on techniques to correct for the effects of mirror sources. It was argued that the "Reflection Cancellor" technique proposed by Guidati et al.⁸ has its limitations for practical use. To overcome the drawbacks, a new "Mirror Minimisation" technique was proposed.

In contrast with the Reflection Cancellor, where the steering vector of the mirror source is added to the original steering vector, the new method leaves the steering vector unchanged. Instead, the source location process is now performed with the extra constraint of low output from the direction of the mirror source. A control mechanism is built in to preserve the robustness of the method.

This new method was successfully applied to phased array measurements in the DNW Low Speed Wind Tunnel LST on a calibration source. The new array processing method proved its capacity to remove the modulations on the free-field spectra.

References

¹Piet, J.F., and Elias, G., "Airframe noise source localization using a microphone array", AIAA Paper 97-1643, 1997.

²Dassen, A.G.M., Sijtsma, P., Holthusen, H., Haaren, E. van, Parchen, R.R., and Looijmans, K.N.H., "The noise of a high-speed train pantograph as measured in the German-Dutch Wind Tunnel DNW", 2nd Int. Workshop on the AeroAcoustics of High-Speed Trains, Berlin, 29/30 April 1997 also TP 97409.

³Dobrzynski, W., Chow, L.C., Guion, P., and Shiells D., "A European study on landing gear airframe noise sources", AIAA Paper 2000-1971, 2000.

⁴Hayes, J.A., Horne, W.C., Soderman, P.T., and Bent, P.H., "Airframe noise characteristics of a 4.7% scale DC-10 model", AIAA paper 97-1594, 1997.

⁵Sijtsma, P., and Holthusen H., "Source location by phased measurements in closed wind tunnel test sections", AIAA Paper 99-1814, 1999 also TP 99108.

⁶Johnson, D.H., and Dudgeon, D.E., *Array Signal Processing*, Prentice Hall, 1993.

⁷Brooks, T.F., and Humphreys Jr., W.M., "Effect of Directional Array Size on the Measurement of Airframe Noise Components", AIAA Paper 99-1958, 1999.

⁸Guidati, S., Brauer, C., and Wagner, S., "The Reflection Cancellor – Phased array measurements in a reverberating environment", AIAA Paper 2002-2462, 2002.

⁹Nelson, P.A., and Yoon, S.H., "Estimation of acoustic source strength by inverse methods: Part I, Conditioning of the inverse problem", *Journal of Sound and Vibration*, Vol. 233, No. 4, pp. 643-668, 2000.

¹⁰Yoon, S.H., and Nelson, P.A., "Estimation of acoustic source strength by inverse methods: Part II, experimental investigation of methods for choosing regularization parameters", *Journal of Sound and Vibration*, Vol. 233, No. 4, pp. 669-705, 2000.

¹¹Oerlemans, S., and Sijtsma, P., "Effects of wind tunnel side-plates on airframe noise measurements with phased arrays", AIAA paper 2000-1938, 2000 also TP 2000-169.

¹²Dougherty, R.P., "Beamforming in acoustic testing", in *Aeroacoustic Measurements*, Ed. T.J. Mueller, Springer, pp. 62-97, 2002.

¹³Harris, F.J., "On the use of windows for harmonic analysis with the discrete Fourier transform", *Proceedings of the IEEE*, Vol. 66, No. 1, pp. 51-83, 1978.

¹⁴Oerlemans, S., and Sijtsma, P., "Determination of absolute levels from phased array measurements using spatial source coherence", AIAA paper 2002-2464, 2002 also TP 2002-226.

¹⁵Cox, H., Zeskind, R.M., and Owen, M.M., "Robust Adaptive Beamforming", *IEEE Proceedings on Acoustics, Speech and Signal Processing*, Vol. ASSP-35, No. 10, pp. 1365-1376, 1987.